Differentially Coherent Detection: Lower Complexity, Higher Capacity?

Yashar Aval, Sarah Kate Wilson* and Milica Stojanovic
Northeastern University, Boston, MA, USA
*Santa Clara University, Santa Clara, CA, USA

***Abstract*—We compare the achievable rate for QPSK and DQPSK modulations while considering the effect of channel estimation errors and pilot overhead. DQPSK is generally regarded in the literature as the low complexity alternative to QPSK, and is considered to sacrifice the performance as a trade-off. This argument is valid when the channel is perfectly known to the receiver. Here, we show that when the cost of pilot overhead and channel estimation errors are considered, there exist cases where DQPSK modulation delivers higher data rates as compared to QPSK modulation, even if optimal ratio of symbols are assigned as pilots. We classify these cases, and show through simulations that they occur frequently in underwater acoustic channels as the long delay spread requires a considerable pilot overhead for estimating the channel. Our results are supported by analysis, as well as simulation.**

I. Introduction

Bit error rate (BER) of quadrature phase shift keying (QPSK) and differential QPSK (DQPSK) modulations have been extensively analyzed in the literature for both additive white Gaussian noise (AWGN) and fading channels. For example, [1] summarize closed form expressions for BER of QPSK and DQPSK modulations for AWGN, Rayleigh, and Rician fading channels. QPSK is shown to outperform DQPSK in all scenarios in terms of the average BER, and that the performance gap shrinks slightly at higher SNRs.

These analyses, however, focus on BER under ideal channel knowledge and ignore the pilot overhead needed for channel estimation. Furthermore, the effect of channel estimation errors needs to be taken into account for making a fair comparison between coherent and differentially coherent detection. Therefore, we focus on the average achievable rate per channel use as the performance metric (which we refer to as the average rate), and consider the effect of both pilot overhead and imperfect channel estimation.

Since detection of DQPSK signals requires very few pilot symbols, it is potentially possible that the pilot overhead and channel estimation errors reduce the achievable rate based on QPSK modulation to less than that of DQPSK. For example, the coherent detection methods designed for underwater channels typically have a significant ratio of carriers designated as pilot and/or null carriers (see e.g. [2], [3]).

We show through numeral evaluations that for QPSK modulation there is tradeoff between DQPSK with no pilots and the loss in rate with coherent channel estimation and QPSK and the related loss in rate due to pilot overhead and channel estimation error. To further this analysis, we find an optimal value for the ratio of pilots to data for different SNR's and the number of taps in the channel.

Finally, we include simulation results based on a fading model for which each arrival path at the receiver evolves over time according to a Rician fading model [4]. The parameters of this model are selected according to the experimentally measured underwater acoustic channels. Simulation results confirm our theoretical observations.

II. System Model

We analyze the average achievable rate per channel use within the framework of an OFDM system. In an OFDM communication system with minimal Doppler spread (compared to carrier spacing), the received signal at the k-th carrier can be modeled as

$$y_k = \sqrt{P} H_k d_k + z_k, \quad (k = 0, \dots, K-1) \tag{1}$$

where d_k is the transmitted data symbol, H_k is the channel coefficient, P is the power allocated to each carrier,[1] y_k is the received signal, and z_k is zero-mean, circularly symmetric Gaussian noise of variance σ_z^2.

We define the carrier SNR as $\mathrm{SNR}_k = P|H_k|^2/\sigma_z^2$. Assuming a normalization of the channel coefficients such that $\mathbf{E}\{|H_k|^2\} = 1$, we define the average SNR as

$$\mathrm{SNR} = \mathbf{E}\{\mathrm{SNR_k}\} = \frac{P}{\sigma_z^2} \tag{2}$$

To find the average achievable rate per channel use for each carrier, we start with specifying the achievable rate per channel use over AWGN channels for QPSK and DQPSK modulations. Note that we assume a block fading model and will average this rate over all possible channel states before averaging over the carriers.

Generally, the achievable rate per channel use for any modulation scheme can be formulated based on the probability density function (PDF) of the decision variable at the receiver. Specifically, for QPSK and DQPSK modulations, without loss of generality (due to symmetry), we can assume that the symbol $d = 1$ is transmitted, resulting in the decision variable $\hat{d}$ at the receiver. If we denote the conditional PDF of this decision variable as $p_{\hat{D}|D}(\hat{d}|1)$, and denote by $P_{\hat{D}}(\hat{d})$ the PDF

[1] We only consider uniform power allocation which is the best practical power allocation policy for underwater acoustic channels [5].

of this decision variable, the achievable rate per channel use is (see [6], [7] for details)[2]

$$R = \int_{\hat{d}} p_{\hat{D}|D}(\hat{d}|1) \log_2 \frac{p_{\hat{D}|D}(\hat{d}|1)}{p_{\hat{D}}(\hat{d})} d\hat{d} \tag{3}$$

where integration is carried over the entire complex plane.

A. Coherent detection (QPSK)

Coherent detection requires channel knowledge, which can be gathered using designated pilot carriers, or in decision directed mode. Here, we focus on pilot-based channel estimation, and assign a fraction α of the carriers as pilots. Insertion of pilot carriers reduces the average rate by the factor $1-\alpha$.

The decision variable for QPSK modulation can be formed as

$$\hat{d}_{k,\mathrm{QPSK}} = \hat{H}_k^* y_k \tag{4}$$

where $\hat{H}_k = H_k + w_k$ is the pilot-based channel estimate, $(.)^*$ denotes complex conjugate operator, and w_k is the channel estimation error. The estimation error is modeled as a zero-mean, circularly symmetric complex Gaussian random variable whose variance, σ_w^2, depends on the SNR, the ratio of carriers designated as pilots, and the estimation method.

An effective channel estimation algorithm for underwater acoustic channels exploits the sparsity of the channel impulse response. For example, if the channel impulse response is dominated by J taps, the estimation error will be (for details see [9])

$$\sigma_w^2 = \frac{J\sigma_z^2}{\alpha K P} \tag{5}$$

The PDF of the decision variable $\hat{d}$ is very difficult to obtain in general. The characteristic function of $\hat{d}$, however, is readily available as a special case of the Gaussian quadratic form (see appendix B of [1] for details),

$$\phi_{\hat{D}}(j\nu) = \frac{1}{2\sigma_z^2\sigma_w^2\nu^2+1} \mathrm{e}^{\frac{|H_k|^2}{2\sigma_z^2\sigma_w^2\nu^2+1}(-(\sigma_w^2+\sigma_z^2)\nu^2+j\nu)} \tag{6}$$

The PDF of the decision variable can be numerically evaluated from its characteristic function and substituted into (3) to evaluate the rate. We refer to this rate as instantaneous rate per carrier, and since it is a function of the channel gain at the k-th carrier, $G_k = |H_k|^2$, we denote it as $R(G_k)$.

B. Differentially Coherent detection (DQPSK)

Differentially coherent detection (e.g. DQPSK) relies on the assumption that the channel coefficients do not change significantly between adjacent carriers, i.e. that $H_k \approx H_{k-1}$.[3]

[2]If the length of the error correction code is limited, the the rate will decrease (see e.g. [8]). However, our focus here is on the *comparison* between QPSK and DQPSK modulations and the limitation on codeword length does not effect the comparison.

[3]Differentially coherent detection can also be applied in the time domain, with similar results as long as there is sufficient coherence between adjacent OFDM blocks. Frequency domain is advantageous, because it simultaneously reinforces the carrier coherence assumption *and* increases the transmission rate

When this assumption holds, the received signal, x_{k-1} acts as the channel estimate,

$$\hat{d}_{k,\mathrm{DQPSK}} = y_{k-1}^* y_k \tag{7}$$

The characteristic function of this decision variable is a special case of (6) where σ_w^2 is replaced by σ_z^2.

C. Rate achievable over Rayleigh block-fading channel

We assume the amplitude of the channel coefficients of all carriers are identically distributed, and follow a Rayleigh distribution. Therefore, the channel gains will follow an exponential distribution,

$$p_G(g) = \mathrm{e}^{-g}, \quad g \geq 0 \tag{8}$$

The average rate per carrier is then evaluated as the expected value of the instantaneous rate,

$$\bar{R}_k = (1-\alpha)\int_0^\infty p_G(g)R(g)dg \tag{9}$$

This integral can be evaluated numerically, and is valid both for QPSK and DQPSK modulations, given that for DQPSK we set $\sigma_w^2 = \sigma_z^2$ and $\alpha = 1/K$. Note that this value for α reflects the fact that one carrier is sacrificed for starting the differentially coherent detection.

The channel gains are identically distributed among carriers. Therefore, the average rate per carrier, $\bar{R}_k$, is the same for all carriers, and the total average rate is,

$$\bar{R} = \frac{1}{K}\sum_{k=0}^{K-1} \bar{R}_k = \bar{R}_k \tag{10}$$

We refer to this quantity as the average rate and consider it to be the performance metric.

III. Results

Fig. 1 shows the average rate as a function of the ratio of designated pilot carriers for QPSK modulation. If we have too few pilot carriers (small α), channel estimation errors limit the performance, while assigning too many pilot carriers reduces the data rate. The circles in this figure point to the optimal pilot ratio which represents the best trade-off between pilot overhead and channel estimation errors.

It can be observed from Fig. 1 that a larger fraction of pilots is needed at lower SNRs. Fig. 2 supports this fact by showing the optimal pilot ratio for multiple values of SNR, as a function of the number of channel taps. Note that the number of pilot carriers must be greater than the number of channel taps for any channel estimation algorithm to converge. This limit is shown in the figure as the dashed line. In the rest of the results, the ratio of pilots are optimally selected (according to SNR, and J) to maximize the rate. This makes a basis for a fair comparison between QPSK and DQPSK modulation.

Fig. 3 compares the average rate for QPSK and DQPSK modulations. When the channel impulse response is dominated by a single tap (e.g. a line of sight channel), QPSK outperforms DQPSK in all SNRs. As the number of channel taps increases, however, channel estimation becomes more

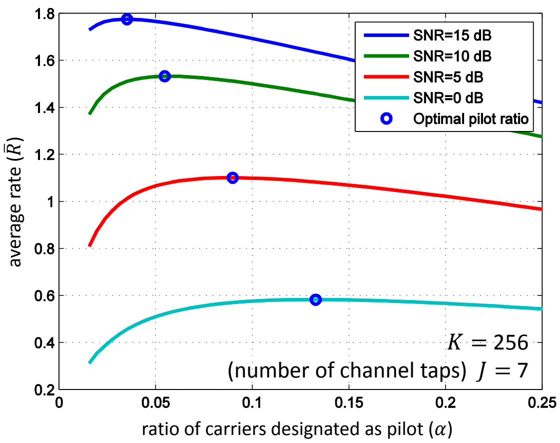

Fig. 1: The average rate (per channel use) for QPSK modulation depends on the ratio α of carriers dedicated as pilots. With too few pilots, the receiver suffers from estimation errors, while assigning too many pilot carriers increases the pilot overhead. The best trade-off is marked with circles for each SNR value.

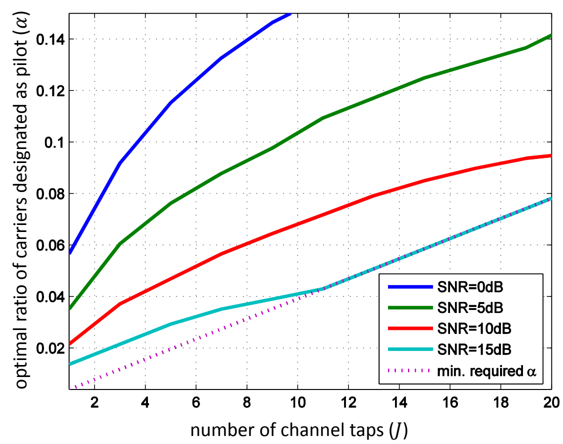

Fig. 2: Optimal ratio of pilot carriers as a function of channel taps. The optimal ratio of pilot carriers depends on the SNR and the number of channel taps. A larger ratio of carriers should be assigned as pilot when the channel has more taps, or when the SNR is low. Also note that at higher SNRs, the optimal number of pilot carriers is dictated by the channel estimation algorithm, which is shown by the dashed line.

challenging, and the number of required pilot carriers grows. Eventually, the cost of channel estimation reduces the average rate of QPSK to below that of DQPSK. The crossing point of the performances is marked with circles.

The crossing point of the performance of QPSK and DQPSK as in Fig. 3 reflects the scenarios where DQPSK outperforms QPSK. Fig. 4 shows this crossing point as a function of SNR. If the channel parameters fall on the right of the curve, DQPSK outperforms QPSK in terms of the average rate.

While Fig. 4 specifies the channel parameters for which DQPSK outperforms QPSK, the question remains to be answered: Where do typical wireless radio and underwater acoustic channels fall in that figure? To answer this question, we normalize the number of channel taps to express it as a fraction of the number of carriers and show the results in Fig. 5. This figure shows that the channel parameters for all wireless radio channels specified in the long-term evolution (LTE) standard including Extended Vehicular A model (EVA) are on the left side of the curve. For underwater acoustic channels, however, the two experimental measurements that are analyzed are located in the region where DQPSK outperforms QPSK.

In addition to the presented theoretical results based on evaluation of (3), we inlude results from simulation. For simulation, we consider a P-path channel in which the path gains h_p and path delays τ_p are chosen at random for each realization of the channel coefficients,

$$H_k = \sum_{p=0}^{P-1} h_p \mathrm{e}^{-j2\pi f_k \tau_p} \tag{11}$$

where f_k represents the frequency of the k-th carrier.

Specifically, we use $P = 7$ paths, and $K = 256$ carrier frequencies spanning the bandwidth between 10 kHz $-$ 15 kHz. The path gains h_p are drawn from independent Rician distributions. The delays are modeled as Gaussian distributed around their nominal value corresponding to the system geometry of [10] with a total delay spread of 5 ms. The simulation consists of 50,000 channel realizations. The average rate per carrier is measured, and averaged across carriers to form the

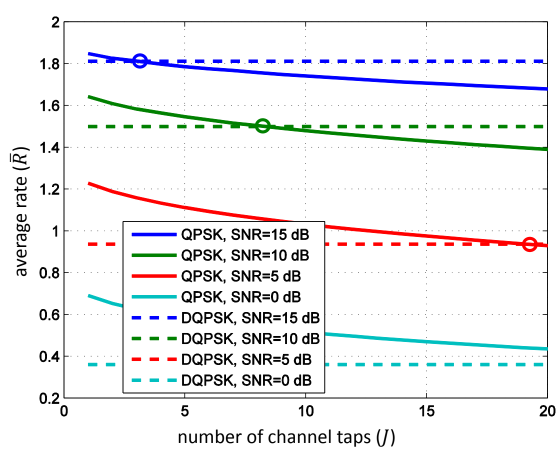

Fig. 3: Average rate for QPSK and DQPSK modulation vs. the number of channel taps. When the channel impulse response is dominated by one tap (flat channel in frequency domain), QPSK delivers the higher rate, regardless of the average SNR. When the number of channel taps increases, however, the average rate of QPSK reduces to less than that of DQPSK. For a given SNR, if the number of channel taps are larger than the crossing point value, QPSK cannot outperform DQPSK with any pilot carrier allocation strategy.

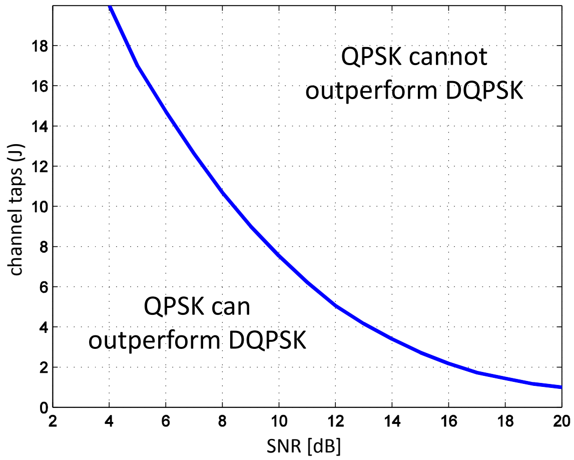

Fig. 4: Scenarios where DQPSK outperforms QPSK. Fig 3 shows that for any SNR, the performance of QPSK and DQPSK modulation cross as the number of channel taps grows. This figure visualizes the crossing point of the performance. If the channel statistics fall on the right hand side of this curve, DQPSK is the clearly the favorable choice as it deliver higher average rate at lower complexity.

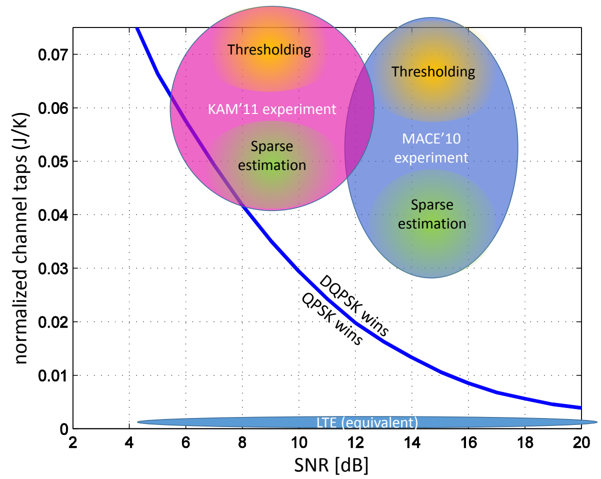

Fig. 5: Parameters of typical wireless and underwater acoustic channels. Although statistics of typical wireless channels do not fall into the region where DQPSK is the clear choice, but most underwater acoustic channels fall in this category.

expected value of the average rate.

The simulation results in Fig. 6 closely resemble our theoretical results. For our simulation, DQPSK outperforms QPSK at SNRs higher than 10 dB. Note, however, that if the ratio of carriers designated as pilots is not selected optimally, DQPSK outperforms QPSK over a wider range of SNRs. For example, if we dedicate 20% of the carriers to pilots, DQPSK will outperform QPSK for SNRs higher than 6 dB.

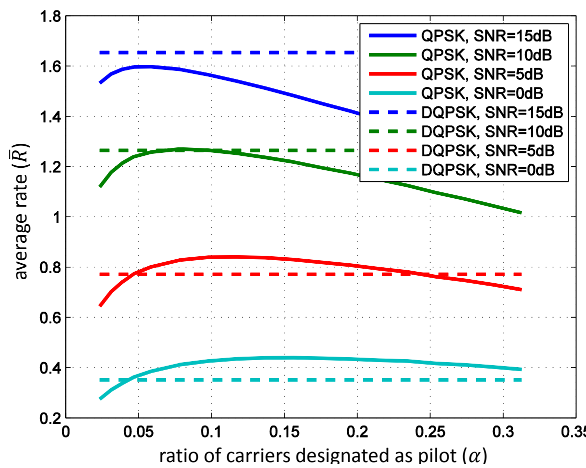

Fig. 6: Results from simulations with parameters taken from experimentally measured underwater acoustic channels. At SNRs higher than 10 dB, DQPSK outperforms QPSK in this simulation, suggesting that for high-SNR underwater acoustic channels, DQPSK is clearly the better choice when compared to QPSK.

IV. Conclusion

We compared the average achievable rate for QPSK and DQPSK both analytically and through simulation. To make a comparison fair, we dedicated an optimal ratio of carriers as pilots according to the channel statistics. Analytical results showed that QPSK does not necessarily outperform DQPSK. In fact, in the cases where the channel impulse response contains a large number of non-zero taps, the cost of channel estimation (pilot overhead and channel estimation errors) can reduce the average rate of QPSK modulation to less than that of DQPSK. This observation is in agreement with the results obtained in [11], [10].

Based on the analytical results, a good example of channels whose parameters are typically in favor of DQPSK, are underwater acoustic channels. Therefore, we repeated the analysis using synthetic data generated based on resemblance to the data collected from a recent underwater acoustic experiment. The simulation data closely resembled the theoretical results.

Future work will include consideration of array receivers, experimental analysis for underwater acoustic channels, and inclusion of higher order constellations in the comparison.

Acknowledgments

This work was supported by the following grants: NSF CNS-1212999, ONR N00014-15-1-2550, and NSF CNS-1428567 .

References

[1] J. G. Proakis and M. Salehi, *Digital Communication*, 5th ed. McGraw-Hill, 2008.

[2] S. Mason, C. Berger, S. Zhou, K. Ball, L. Freitag, and P. Willett, "An OFDM design for underwater acoustic channels with doppler spread," in *5th IEEE Sig. Proc. Educ. Workshop*, Jan 2009, pp. 138–143.

[3] B. Li, S. Zhou, M. Stojanovic, L. Freitag, J. Huang, and P. Willett, "MIMO-OFDM over an underwater acoustic channel," in *OCEANS 2007*, Sept 2007, pp. 1–6.

[4] P. Qarabaqi and M. Stojanovic, "Statistical characterization and computationally efficient modeling of a class of underwater acoustic communication channels," *IEEE J. of Ocean. Eng.*, vol. 38, no. 4, pp. 701–717, Oct 2013.
[5] Y. Aval, S. Wilson, and M. Stojanovic, "On the achievable rate of a class of acoustic channels and practical power allocation strategies for OFDM systems," *Oceanic Engineering, IEEE Journal of*, vol. 40, no. 4, pp. 785–795, Oct 2015.
[6] G. Ungerboek, "Channel coding with multilevel/phase signals," *IEEE Trans. on Info. Theory*, 1982.
[7] R. G. Gallager, *Information Theory and Reliable Communication*. Wiley, 1968.
[8] Y. Polyanskiy, H. Poor, and S. Verdu, "Channel coding rate in the finite blocklength regime," *IEEE Trans. on Info. Theory*, vol. 56, no. 5, pp. 2307–2359, May 2010.
[9] M. Morelli and U. Mengali, "A comparison of pilot-aided channel estimation methods for OFDM systems," *IEEE Trans. on Sig. Proc.*, vol. 49, no. 12, pp. 3065–3073, Dec. 2001.
[10] Y. M. Aval and M. Stojanovic, "Differentially coherent multichannel detection of acoustic OFDM signals," *IEEE J. of Ocean. Eng.*, vol. 40, no. 2, pp. 251–268, Apr. 2015.
[11] S. Lu and N. Al-Dhahir, "Coherent and differential ICI cancellation for mobile OFDM with application to DVB-H," *IEEE Trans. on Wireless Commun.*, vol. 11, no. 12, Nov. 2008.